frontiers in
PLANT SCIENCE

ORIGINAL RESEARCH ARTICLE
published: 31 October 2011
doi: 10.3389/fpls.2011.00071

Mutations in an atypical TIR-NB-LRR-LIM resistance protein confer autoimmunity

Dongling Bi[1†], Kaeli C. M. Johnson[2,3†], Zhaohai Zhu[1], Yan Huang[2,3], Fang Chen[1], Yuelin Zhang[1] and Xin Li[2,3]*

[1] National Institute of Biological Sciences, Beijing, China
[2] Michael Smith Laboratories, University of British Columbia, Vancouver, BC, Canada
[3] Department of Botany, University of British Columbia, Vancouver, BC, Canada

Edited by:
Ken Shirasu, University of California Davis, USA

Reviewed by:
Walter Gassmann, University of Missouri, USA
Melanie Sacco, California State University Fullerton, USA

***Correspondence:**
Xin Li, Department of Botany, University of British Columbia, 2185 East Mall, Vancouver, BC, Canada V6T1Z4.
e-mail: xinli@msl.ubc.ca

[†]Dongling Bi and Kaeli C. M. Johnson have contributed equally to this work.

In order to defend against microbial infection, plants employ a complex immune system that relies partly on resistance (R) proteins that initiate intricate signaling cascades upon pathogen detection. The resistance signaling network utilized by plants is only partially characterized. A genetic screen conducted to identify novel defense regulators involved in this network resulted in the isolation of the *snc6-1D* mutant. Positional cloning revealed that this mutant contained a molecular lesion in the *chilling sensitive 3* (*CHS3*) gene, thus the allele was renamed *chs3-2D*. *CHS3* encodes a TIR-NB-LRR R protein that contains a C-terminal zinc-binding LIM (Lin-11, Isl-1, Mec-3) domain. Although this protein has been previously implicated in cold stress and defense response, the role of the LIM domain in modulating protein activity is unclear. The *chs3-2D* allele contains a G to A point mutation causing a C1340 to Y1340 substitution close to the LIM domain. It encodes a dominant gain-of-function mutation. The *chs3-2D* mutant is severely stunted and displays curled leaf morphology. Additionally, it constitutively expresses *PATHOGENESIS-RELATED* (*PR*) genes, accumulates salicylic acid, and shows enhanced resistance to the virulent oomycete isolate *Hyaloperonospora arabidopsidis* (*H.a.*) Noco2. Subcellular localization assays using GFP fusion constructs indicate that both CHS3 and chs3-2D localize to the nucleus. A third *chs3* mutant allele, *chs3-3D*, was identified in an unrelated genetic screen in our lab. This allele contains a C to T point mutation resulting in an M1017 to V1017 substitution in the LRR–LIM linker region. Additionally, a *chs3-2D* suppressor screen identified two revertant alleles containing secondary mutations that abolish the mutant morphology. Analysis of the locations of these molecular lesions provides support for the hypothesis that the LIM domain represses CHS3 R-like protein activity. This repression may occur through either autoinhibition or binding of a negative defense regulator.

Keywords: innate immunity, *Arabidopsis*, resistance protein, CHS3, LIM domain

INTRODUCTION

In order to evade pathogen infection plants have developed complex resistance mechanisms. Conserved pathogen features necessary for the microbial lifestyle, collectively known as pathogen-associated molecular patterns (PAMPs), can be recognized by pattern recognition receptors on the plant cell surface (Zipfel and Felix, 2005). PAMP detection elicits a signaling cascade leading to the activation of PAMP-triggered immunity (PTI; Jones and Dangl, 2006). However, during the process of infection successful pathogens are able to release effector molecules into the plant host cell that can inhibit PTI, attenuating defense responses. To compensate, plants have evolved many *RESISTANCE* (*R*) genes encoding proteins that can recognize these effector molecules, thereby rapidly and effectively inducing defense responses to prevent the spread of infection. These responses may include the accumulation of the defense hormone salicylic acid (SA), induction of *PATHOGENESIS-RELATED* (*PR*) genes, production of reactive oxygen species (ROS), reinforcement of the cell wall, and a type of localized cell death referred to as the hypersensitive response (HR; Hammond-Kosack and Jones, 1996).

The majority of plant R proteins possess a central nucleotide-binding (NB) site, a number of leucine-rich repeats (LRRs) at the C terminus, and either a coiled-coil (CC) or Toll/interleukin1-receptor-like (TIR) domain at the N terminus (Dangl and Jones, 2001). There are roughly 150 *R* genes encoding NB-LRR proteins distributed throughout the *Arabidopsis* genome (Meyers et al., 2003). Signaling through many CC-NB-LRR R proteins requires NON-SPECIFIC DISEASE RESISTANCE 1 (NDR1) as an intermediate (Aarts et al., 1998), while signaling through most TIR-NB-LRR R proteins typically involves ENHANCED DISEASE SUSCEPTIBILITY 1 (EDS1), PHYTOALEXIN-DEFICIENT 4 (PAD4), and SENESCENCE-ASSOCIATED GENE 101 (SAG101; Feys et al., 2005). These pathways appear to later converge and result in the deployment of similar defense mechanisms.

One key step in resistance signaling is the accumulation of the defense hormone SA. Downstream of SA synthesis, NON-EXPRESSOR OF PATHOGENESIS-RELATED GENES 1 (NPR1) functions as an essential positive regulator of resistance (Cao et al., 1994; Rairdan and Delaney, 2002). Through its interactions with the TGA family of basic leucine zipper transcription

factors, NPR1 modulates the expression of *PR* genes (Dong, 2004). The *npr1-1* mutation abolishes SA-induced *PR* gene expression and pathogen resistance, and does not induce the expression of the *pPR2-GUS* reporter gene (Cao et al., 1994). Thus, a suppressor screen to identify negative regulatory components involved in resistance signaling can be carried out in the *npr1* genetic background quite simply by using *pPR2-GUS* reporter gene expression for mutant isolation. Early screens resulted in the identification of *SUPPRESSOR OF NPR1, INDUCIBLE 1* (*SNI1*), *SUPPRESSOR OF NPR1, CONSTITUTIVE 1* (*SNC1*), *SUPPRESSOR OF SALICYLIC ACID INSENSITIVE* (*SSI*) genes, and *SUPPRESSOR OF NIM1-1* (*SON1*; Li et al., 1999, 2001; Shah et al., 1999, 2001; Kim and Delaney, 2002; Shirano et al., 2002). Recent independent screens have led to the identification of *SNC2*, *SNC3*, *SNC4*, and *SNC5* (renamed *SUPPRESSOR OF RPS4-RLD*; *SRFR1*) as intermediates in plant pathogen resistance (Bi et al., 2010; Li et al., 2010; Zhang et al., 2010).

In this study, we report the identification and characterization of a *snc6-1D* mutant isolated from an *npr1-1* suppressor screen. *SNC6* encodes *CHS3*, a TIR-NB-LRR protein with an additional LIM (Lin-11, Isl-1, Mec-3; Freyd et al., 1990) domain at the C terminus. Thus, *snc6-1D* was renamed *chs3-2D*. The *chs3-2D* mutant is dwarfed and displays curled leaf morphology. It constitutively induces the expression of *PR* genes, shows enhanced oomycete resistance, and accumulates SA. Two revertant mutants were isolated through a *chs3-2D* suppressor screen. Another gain-of-function mutant allele, *chs3-3D*, has also been identified in our lab as part of an independent *mos4 (modifier of snc1, 4)* suppressor screen. Analysis of the locations of these mutations provides further insight into the structural and functional details of the different domains of this unique R-like protein.

RESULTS

IDENTIFICATION AND GENETIC CHARACTERIZATION OF THE *snc6-1D npr1-1* MUTANT

In plants, NPR1 is an essential regulatory component that functions downstream of salicylic acid (SA) induction in the systemic acquired resistance (SAR) pathway (Dong, 2004). In order to identify novel negative defense regulators independent of NPR1, a suppressor screen (described previously by Gao et al., 2008) was carried out in the *npr1-1* background. The *snc6-1D npr1-1* mutant was identified by its constitutive expression of *pPR2-GUS* (**Figure 1A**). When the *snc6-1D npr1-1* mutant (with *pPR2-GUS*) was backcrossed with *SNC6 npr1-1* (with *pPR2-GUS*), the F1 progeny displayed the mutant morphology and constitutively expressed the *pPR2-GUS* reporter gene (data not shown), indicating that *snc6-1D* is a dominant mutation. Additionally, the *snc6-1D npr1-1* mutant displays dwarfed morphology and curled leaves (**Figure 1B**). These morphological traits are similar to but much more severe than those observed in the autoimmune *R* gene mutant *snc1* (Li et al., 2001).

PR GENE EXPRESSION AND PATHOGEN RESISTANCE IN *snc6-1D npr1-1*

In *snc6-1D npr1-1*, constitutive *pPR2-GUS* reporter gene expression was observed primarily in the leaves and petioles (**Figure 1A**). The induction of *pPR2-GUS* likely occurs via an NPR1-independent pathway in this mutant. When the expression levels of endogenous *PR1* and *PR2* were examined using RT-PCR analysis, both *PR* genes showed constitutively enhanced expression in *snc6-1D npr1-1* (**Figures 1C,D**).

The biotrophic oomycete *Hyaloperonospora arabidopsidis* (*H.a.*) is virulent on wild type *Arabidopsis* plants. Upon infection with *H.a.* isolate Noco2, the *snc6-1D npr1-1* mutant supported ∼50 times less oomycete growth than wild type and *npr1-1* plants (**Figure 1E**). Therefore, in keeping with the observed constitutive *PR* gene expression, the *snc6-1D* mutation activates constitutive disease resistance in the *npr1-1* background.

SA ACCUMULATION IN *snc6-1D npr1-1*

The dwarfed size and curled leaf phenotypes observed in the *snc6-1D npr1-1* mutant, similar to those displayed in *snc1* plants, are typical of plants with elevated SA levels (Bowling et al., 1997). High-pressure liquid chromatography was used to measure the endogenous levels of both free SA and salicylic acid β-glucoside (SAG), the storage form of the defense hormone that enables the release of free SA as required by the plant. Levels of free SA were ∼5 times higher in *snc6-1D npr1-1* than in wild type or *npr1-1*, and levels of total SA (SA + SAG) were ∼25 times higher than in wild type and ∼5 times higher than in *npr1-1* (**Figure 1F**). SA accumulation observed under uninduced conditions in *snc6-1D npr1-1* is likely partly responsible for the constitutive *PR* gene expression and disease resistance observed in the mutant.

MAP-BASED CLONING OF THE *snc6-1D* LOCUS

To map the *snc6-1D* locus, *snc6-1D npr1-1* (Col-0 ecotype) was crossed with wild type (*SNC6 NPR1*) L*er* ecotype. Rough mapping showed the *snc6-1D* mutation is located on the top of chromosome 5 between markers T24H18 and F17K4. Further fine mapping narrowed the location of the mutation between markers MPI7 and MRG7, an interval of approximately 120 kb (**Figure 2A**).

Sequencing of PCR fragments covering this region revealed a single G to A point mutation in the fifth exon of *At5g17890* (**Figure 2B**). A mutation in this gene had previously been identified and characterized in a screen for temperature sensitive mutants, and the gene was named *CHILLING SENSITIVE 3* (*CHS3*; Yang et al., 2010). Thus, the *snc6-1D* allele was renamed *chs3-2D*. *CHS3* is predicted to encode a protein of 1613 amino acids containing TIR, NB, LRR, and LIM domains (**Figure 5B**). The *chs3-2D* mutation results in a C1340 to Y1340 substitution close to the LIM domain. Since *chs3-2D* is dominant, we hypothesized this might be a gain-of-function mutation.

chs3-2D IS A GAIN-OF-FUNCTION MUTATION

To determine the genetic nature of the *chs3-2D* mutation, wild type plants were transformed with either *CHS3-GFP* or *chs3-2D-GFP* fusion constructs under the control of its endogenous promoter. When transformed with *CHS3-GFP*, the transformants displayed wild type morphology, *PR* gene expression, and *H.a.* Noco2 resistance (two independent representative lines are shown in **Figures 3A–D**). In contrast, lines transformed with *chs3-2D-GFP* displayed mutant morphology, constitutive *PR* gene expression and enhanced resistance to *H.a.* Noco2. This indicates that *chs3-2D* is a gain-of-function mutation resulting in constitutive disease resistance. Although *chs3-2D-GFP* is able to confer autoimmunity, we were not able to observe the GFP signal of the fusion

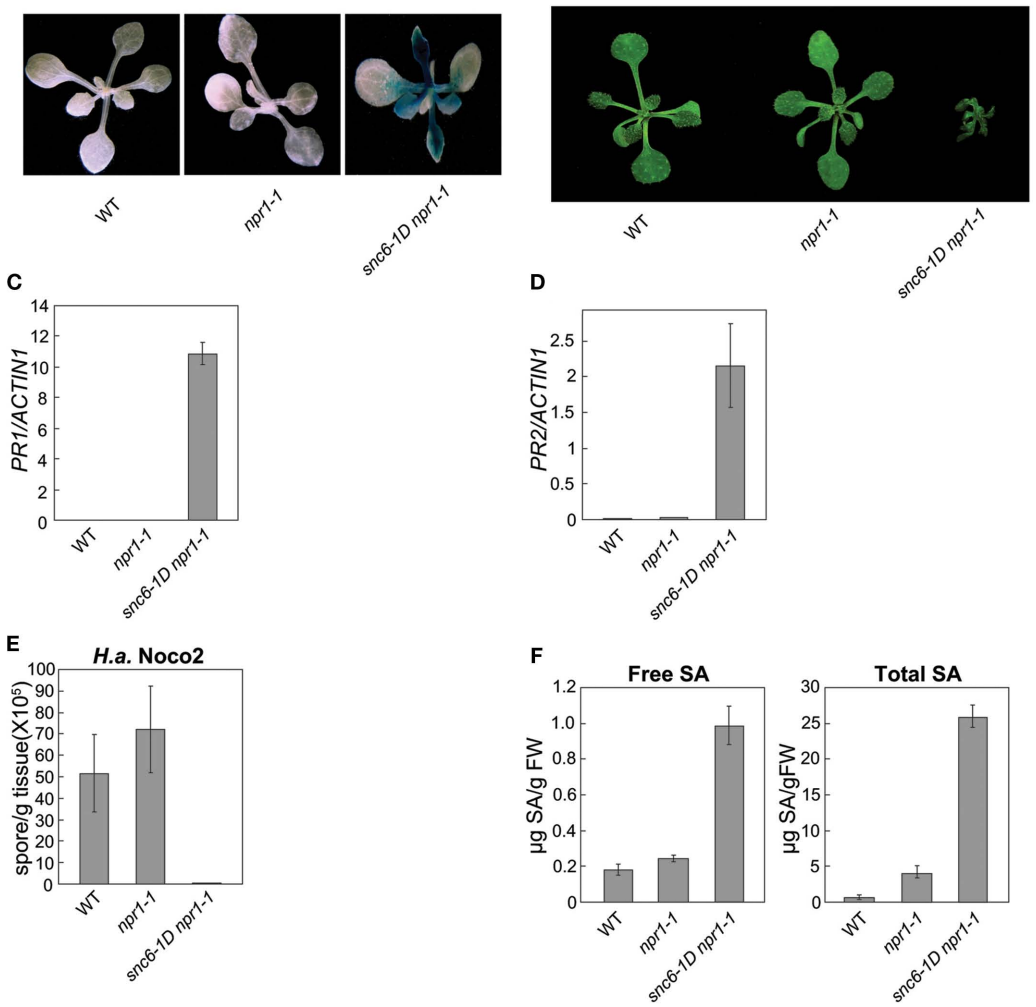

FIGURE 1 | Phenotypic characterization of *snc6-1D npr1-1*. **(A)** Expression of the *pPR2-GUS* reporter gene, present in wild type (WT) and *npr1-1* mutant background, in WT, *npr1-1*, and *snc6-1D npr1-1* plants. Seedlings were grown on MS media for 14 days prior to staining for GUS activity. The three photographs shown were taken at different magnifications in order to effectively capture GUS staining, thus seedling size should not be compared between panels. **(B)** Morphology of wild type (WT), *npr1-1*, and *snc6-1D npr1-1* plants. Representative 4-week-old soil-grown plants were photographed. **(C,D)** Endogenous expression of **(C)** *PR1* and **(D)** *PR2* relative to *Actin 1* in WT, *npr1-1*, and *snc6-1D npr1-1*. Values presented are averages of three replicates ± SD. **(E)** Growth of *H.a.* Noco2 on WT, *npr1-1*, and *snc6-1D npr1-1* mutants 7 days post-infection. Values presented are averages of three replicates ± SD. **(F)** Endogenous free and total SA levels in WT, *npr1-1*, and *snc6-1D npr1-1*. Plants were grown on soil for 4 weeks and leaf tissue was collected for SA extraction. SA levels were analyzed using high-pressure liquid chromatography. Values presented are averages of four replicates ± SD.

protein in transgenic plants, probably due to the very low protein levels.

CHS3 AND chs3-2D LOCALIZE TO THE NUCLEUS

Nuclear localization of CHS3 is suggested by WoLFpSORT, although the PredictProtein program indicates that the protein does not contain a known nuclear localization signal (Rost et al., 2003; Horton et al., 2007). To experimentally examine the subcellular localization of CHS3, *Arabidopsis* mesophyll protoplasts were transformed with either *CHS3-GFP* or *chs3-2D-GFP* fusion constructs. GFP fluorescence was detected exclusively in the nucleus of protoplasts for both constructs (**Figure 4**). No obvious differences in GFP fluorescence subcellular localization were observed.

IDENTIFICATION OF ADDITIONAL *chs3* ALLELES

A *chs3-2D* suppressor screen was undertaken to find mutant alleles causing a reversion to wild type morphology. Two revertant *chs3* alleles were identified (**Figure 5A**). Sequence analysis revealed that the first allele, *chs3-2D-r1*, contains a C to T point mutation in the LRR domain resulting in an L716 to F716 substitution while the second allele, *chs3-2D-r1*, has a G to A point mutation in the LRR–LIM linker region that causes an E1007 to G1007 substitution. An additional *chs3* gain-of-function allele, *chs3-3D*, was identified from a separate *mos4* suppressor screen undertaken in our lab (the *mos4* suppressor screen will be described in future publications). Similar to *chs3-2D*, the *chs3-3D* mutant displays a dwarf, curled leaf phenotype and constitutively expresses the *pPR2-GUS*

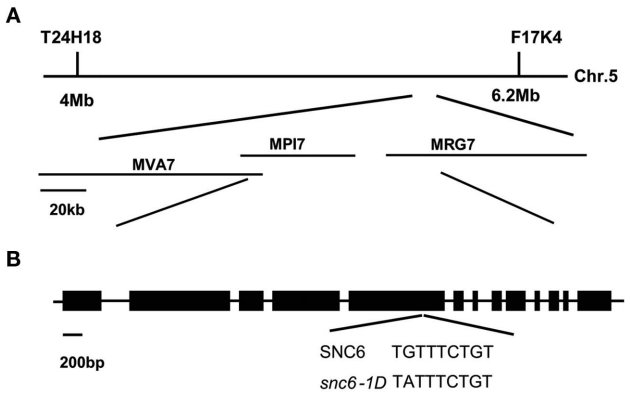

FIGURE 2 | Map-based cloning of the *snc6* locus on chromosome 5. (A) A genetic map of the region of chromosome 5 containing the *SNC6* locus, with markers used for mapping indicated. **(B)** Gene structure of *SNC6* (*At5g17890*, previously named *CHS3*) and the position of the molecular lesion in *snc6-1D*/*chs3-2D*. Boxes and lines represent exons and introns, respectively.

reporter gene (**Figure A1** in Appendix). This allele contains a C to T point mutation in the LRR–LIM linker region that causes an M1017 to V1017 substitution. The locations of these mutations are presented along with the locations of the *chs3-1* (Yang et al., 2010) and *chs3-2D* mutations (**Figure 5B**).

DISCUSSION

The *chs3-2D* mutation characterized in this study was shown to suppress the enhanced disease susceptibility phenotypes of *npr1-1* through the activation of constitutive defense responses. The *chs3-2D npr1-1* double mutant displayed dwarfed, curled leaf morphology similar to that of *snc1*, a well characterized autoimmune mutant. Additionally, *chs3-2D npr1-1* constitutively expressed the *pPR2-GUS* reporter construct as well as endogenous *PR1* and *PR2*, and accumulated the defense hormone SA. The molecular lesion responsible for these mutant phenotypes is located close to the C-terminal LIM domain of the CHS3 R-like protein, and was shown to be a gain-of-function mutation. The mutation does not seem to alter the nuclear localization of the protein. Two revertant alleles were isolated and an additional gain-of-function mutant allele (*chs3-3D*) was identified in separate genetic screens. The mutation sites in these gain-of-function and loss-of-function alleles provide further understanding as to the potential function of the enigmatic LIM domain of CHS3.

chs3-2D MUTANT PHENOTYPES SUBTLY DIFFER FROM THOSE OF *chs3-1*, *chs2*/*rpp4*, AND *ssi4*

The *chs3-1* mutant exhibits enhanced freezing tolerance and constitutive resistance against *Pseudomonas syringae* pv. *tomato* (*Pst*) DC3000 when grown at 16°C, yet when grown at 22°C these phenotypes are mitigated (Yang et al., 2010). Another chilling sensitive R protein mutant, *chs2*, contains a dominant point mutation in the NB–ARC1 domain of *RPP4* (Huang et al., 2010). Like *chs3-1*, the gain-of-function resistance phenotypes of this mutant are only observable at temperatures below 16°C. Similarly, the *chs3-2D*

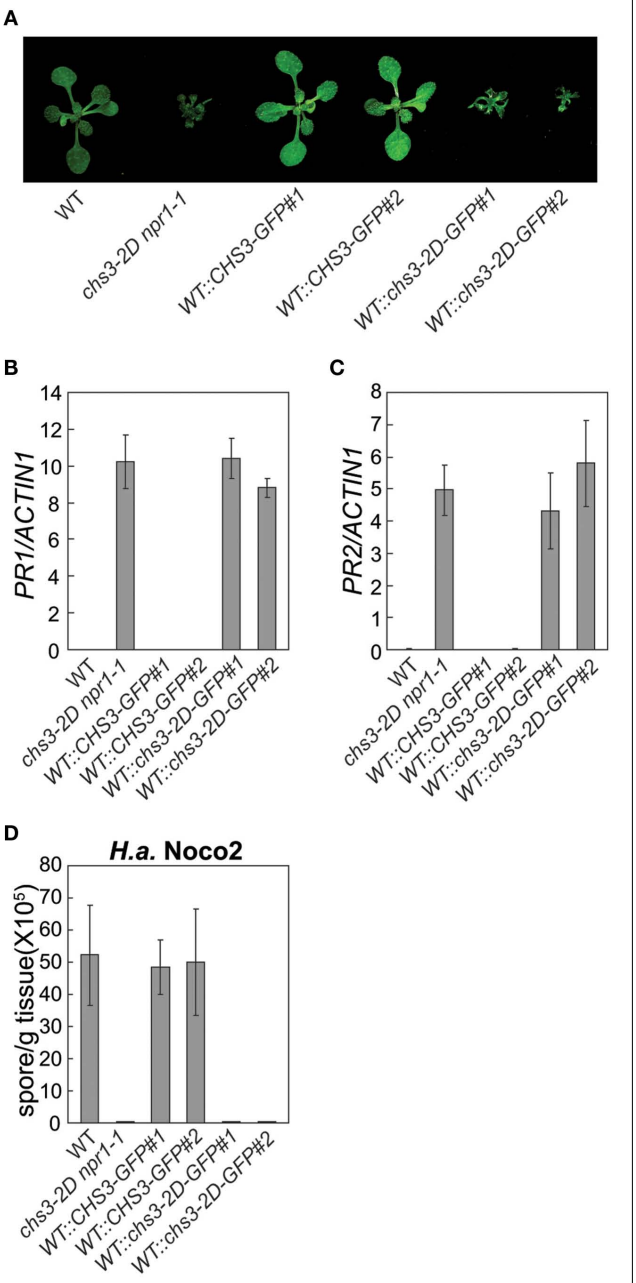

FIGURE 3 | Characterization of transgenic plants expressing *CHS3-GFP or chs3-2D-GFP* under the control of its endogenous promoter. **(A)** Morphology of wild type (WT), *chs3-2D npr1-1*, *CHS3-GFP*line 1, *CHS3-GFP*line 2, *chs3-2D-GFP*line 1, and *chs3-2D-GFP*line 2 soil-grown plants. *CHS3-GFP* and *chs3-2D-GFP* constructs were expressed in the WT Col-0 background. Representative plants were photographed 4 weeks after germination. **(B,C)** Endogenous expression of **(B)** *PR1* and **(C)** *PR2* relative to *Actin 1* in the above-mentioned genotypes. Values presented are averages of three replicates ± SD. **(D)** Growth of *H.a.* isolate Noco2 on the above-mentioned genotypes 7 days post-infection. Values presented are averages of three replicates ± SD.

npr1-1 morphological phenotypes are temperature sensitive, with mutant plants displaying acute stunting when grown at 16°C (data

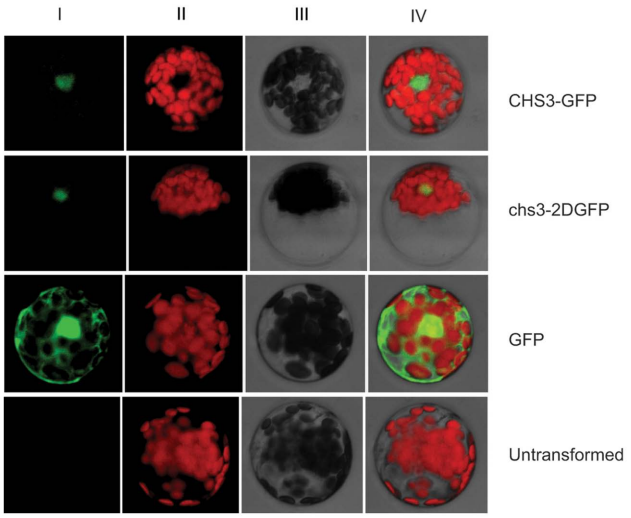

FIGURE 4 | CHS3-GFP and chs3-2D-GFP localize to the nucleus. CHS3-GFP and chs3-2D-GFP fluorescence as observed by confocal microscopy in *Arabidopsis* mesophyll protoplast cells (I: GFP, II: Autofluorescence, III: Bright field, IV: Merged). Experiments were repeated with multiple cells for each construct.

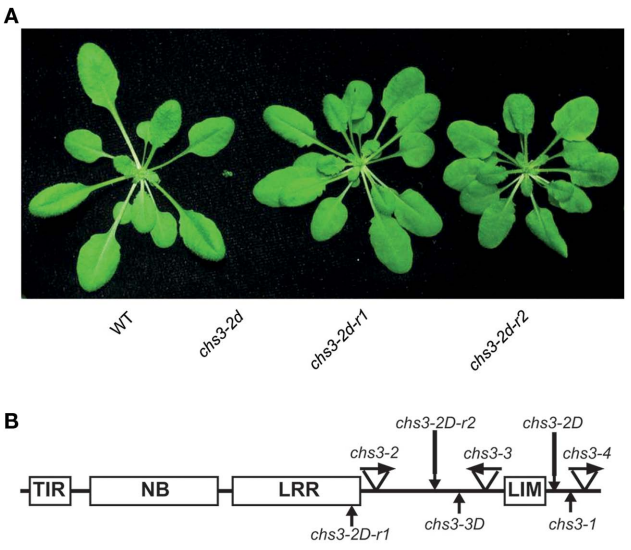

FIGURE 5 | Identification of *chs3-2D* revertants and location of a number of *chs3* mutations. (A) Morphology of WT, *chs3-2D npr1-1*, *chs3-2D-r1*, and *chs3-2D-r2* soil-grown plants. Representative plants were photographed 4 weeks after germination. **(B)** Predicted CHS3 protein structure and locations of *chs3-1* (Yang et al., 2010), *chs3-2D*, *chs3-3D*, *chs3-2D-r1*, and *chs3-2D-r2* mutations. TIR, Toll/Interleukin-1-receptor-like; NB, nucleotide-binding site; LRR, leucine-rich repeat; LIM, Lin-11, Isl-1, and Mec-3 domain. Arrows indicate the locations of the point mutations corresponding to *chs3* mutations.

not shown). However, constitutive disease resistance is maintained in *chs3-2D npr1-1* mutant plants grown at 22˚C (**Figure 1**). As well, the *chs3-1* mutation is recessive in the Col-0 background while the *chs3-2D* mutation is dominant, which is more typical of gain-of-function mutations. These data indicate that *chs3-2D* is a more severe gain-of-function allele of *CHS3*. The *chs3-2D* allele may be of use in future genetic studies of resistance signaling as its constitutive defense response phenotypes are more stable, exhibited at both 16 and 22˚C (data not shown).

The *ssi4* mutant identified in an earlier *npr1* suppressor screen displays an autoimmune phenotype similar to that of *chs3-2D*, caused by a semi-dominant point mutation in the NB domain of a TIR-NB-LRR R protein (Shirano et al., 2002). However, rather than displaying chilling sensitivity, this mutant is sensitive to humidity; at a relative humidity of 95%, the dwarfed size and constitutive resistance associated with this mutation are abolished (Zhou et al., 2004). Taken together with the chilling sensitive mutants, this indicates that disease resistance and environmental stress response pathways are intricately tied in plants, although the degree of overlap and the precise signaling events required for each pathway remain unclear.

CHS3 IS A NUCLEAR PROTEIN

Wild type CHS3 fused to GFP localizes to the nucleus, and this subcellular localization is unaltered by the *chs3-2D* mutation (**Figure 4**). This is not a surprising finding as a number of R proteins, including barley Mla10, tobacco N, and *Arabidopsis* RPS4 and SNC1, have been shown to localize to the nucleus, although in some cases nuclear localization requires the presence of effector proteins (Burch-Smith et al., 2007; Shen et al., 2007; Wirthmueller et al., 2007; Cheng et al., 2009). As well, a number of LIM proteins localize to the nucleus (reviewed in Kadrmas and Beckerle, 2004). The expression of the *CHS3-GFP* fusion construct in the Col-0 wild type background confers wild type resistance, whereas *chs3-2D-GFP* expressed in the wild type background confers constitutive defense response induction (**Figure 3**). The constitutive resistance phenotypes observed in the *chs3-2D-GFP* transgenic plants provide further evidence that this protein is correctly localized. The lack of observable GFP fluorescence in transgenic plants indicates that CHS3-2D is of very low abundance but likely has high defense activation activity. We did not observe differences in localization in the protoplast system between wild type and chs3-2D-GFP. However, that does not exclude the possibility that in plants quantitative localization differences contribute to differences in defense response activation.

INSIGHTS INTO LIM DOMAIN FUNCTION

CHS3 belongs to the TIR-NB-LRR subclass of R proteins. In terms of R protein functionality, the presence of the N-terminal TIR domain determines which downstream intermediates will be involved in resistance signaling (Feys et al., 2005). Studies of the flax L6 R protein show that the TIR domain self-associates, likely forming a homodimer, and is required for resistance signaling (Bernoux et al., 2011). The TIR domain has also been implicated in the induction of the cell death response (Frost et al., 2004; Weaver et al., 2006; Swiderski et al., 2009). Likewise, the NB domain appears to play a critical role in resistance signaling and the provocation of cell death (Rairdan et al., 2008). It acts in concert with the ARC1 and ARC2 subdomains to bind nucleotides, and by this means regulates R protein activity (Tameling et al., 2006). Effector

recognition specificity possibly derives from LRR domain diversity (Ellis et al., 1999; Dodds et al., 2001; Shen et al., 2003; Rairdan and Moffett, 2006). Intramolecular interactions between the different domains are believed to be crucial for precise R protein functionality (Rairdan and Moffett, 2006).

The N terminus and LRR domain are thought to be involved in the regulation of localized cell death, as suggested by domain swap experiments between tomato R protein homologs Mi-1.1 and Mi-1.2 (Hwang et al., 2000). Studies on Rx, a *Solanum tuberosum* R protein required for resistance to Potato Virus X, found that autoactivation was conferred upon deletion of the LRR domain or by specific point mutations in the LRR or NB domains (Bendahmane et al., 2002). Domain swap experiments between Rx and the homologous R protein Gpa2 indicate that interactions between the LRR and ARC2 domains may be required for autoinhibition of the R protein in the absence of a pathogen (Rairdan and Moffett, 2006). These experiments set a precedent for the repression of R protein activity via intramolecular interactions. While the detailed functional roles of the above domains are still being elucidated, comparatively little is known about the additional C-terminal LIM domain possessed by CHS3.

Genes encoding LIM domain-containing proteins have been identified in all well-studied eukaryotic genomes, yet most domain characterization studies have been done in animals. While early experiments demonstrated LIM domain-specific DNA-binding activity *in vitro* (Baltz et al., 1996; Nishiya et al., 1998), LIM domains are thought to serve primarily as protein–protein interaction interfaces and are involved in dimerization (Feuerstein et al., 1994; Schmeichel and Beckerle, 1994; Arber and Caroni, 1996). Animals possess a large number of diverse LIM proteins that have been implicated in a variety of biological processes, including the regulation of actin organization, axon guidance, cell-fate determination, and cell signaling (reviewed in Kadrmas and Beckerle, 2004). Plants contain fewer LIM proteins, and in *Arabidopsis* LIM proteins are encoded by genes from two distinct subfamilies. The first consists of six genes encoding proteins with two LIM domains that are homologous to animal CRP proteins (Eliasson et al., 2000). These proteins bind actin filaments and regulate actin cytoskeleton organization (Papuga et al., 2010). The genes in the second subfamily encode DA1 and seven DA1-related (DAR) proteins, including CHS3 (DAR4), which are plant-specific proteins each containing a single conserved LIM domain (Li et al., 2008). While DA1 is involved in seed and organ size regulation and CHS3 is associated with resistance signaling and cold response (Yang et al., 2010), the role of the LIM domain in modulating these activities remains ambiguous.

The locations of the constitutive resistance-inducing *chs3* mutations provide some insight. The *chs3-1* allele carries a point mutation in an intron–exon junction in a domain of unknown function close to the LIM domain, possibly resulting in a truncated protein due to splicing discrepancies (Yang et al., 2010). The *chs3-2D* mutation is caused by a C1340 to Y1340 substitution close to the LIM domain. Additionally, a *chs3-3D* mutation identified in an unrelated *mos4* suppressor screen results from an M1017 to V1017 substitution in the LRR–LIM linker region (**Figure 5**). The distribution of these mutations throughout a number of domains highlights the importance of the C terminus in regulating R-like activity in CHS3. The entire C terminus may be required for autoinhibition, with the regions surrounding the LIM domain playing an essential role in maintaining correct folding of the LIM to confer proper repression. On the other hand, repression may be a result of binding to a negative regulator. The mutation sites may all be located in close proximity in the three-dimensional protein, perhaps as part of a binding site for an interacting repressor protein.

The mutation sites resulting in a reversion to wild type morphology in *chs3-2D* mutant plants give pause for thought. One revertant contains an L716 to F716 substitution in the LRR domain. Due to the complex intramolecular interactions between the TIR, NB, and LRR domains required for R protein activation, this mutation may result in loss of R protein activity. The other revertant allele contains a G to A point mutation that causes an E1007 to G1007 substitution in the LRR–LIM linker region, in close proximity to the *chs3-3D* molecular lesion. Plants heterozygous for either *chs3-2D-r1* or *chs3-2D-r2* in the *chs3-2D* background exhibit an intermediate morphological phenotype (data not shown), indicating that these mutations are semi-dominant. This is similar to what was observed for the *CHS3* loss-of-function T-DNA insertion alleles *chs3-2*, *chs3-3*, *chs3-4* (**Figure 5B**; Yang et al., 2010), thus providing support for *chs3-2D-r1* and *chs3-2D-r2* being loss-of-function mutations as well. A similar *R* gene dosage effect has been observed in plants heterozygous for the *snc1* mutant, as the stunted morphological trait is recessive while the constitutive *PR* gene expression trait is semi-dominant (Li et al., 2001).

It is possible that the gain-of-function mutations surrounding the LIM release the self-inhibition of the LIM motif while certain loss-of-function mutations enhance its repressive activity through their different impacts on protein structure and conformation. Alternatively, these mutations may have opposing effects on protein-binding sites. The gain-of-function mutations may weaken binding platforms for negative regulators, while certain loss-of-function mutations may stabilize these interaction sites. It is also possible that the revertant mutations result in a loss of constitutive defense response activation simply by destabilizing the CHS3 protein or disrupting the whole protein structure leading to complete loss-of-function of the protein.

A PUTATIVE MODEL FOR LIM FUNCTIONALITY

Yang et al. (2010) previously hypothesized that the LIM domain acts to repress R protein activity in CHS3 in the absence of pathogenic effector molecules through intramolecular interactions. Indeed, intramolecular autoinhibitory activity of the LIM domain has been observed with a number of animal LIM proteins (Nagata et al., 1999; Garvalov et al., 2003), and as stated above autoinhibition of R protein activity via intramolecular interactions has been observed in Rx (Rairdan and Moffett, 2006). The unique LIM domain of CHS3 may add another layer of complexity to this self-regulation. Thus, in one proposed model for LIM domain regulation of CHS3 R protein activity, the LIM domain binds directly to the N terminus of CHS3 in the absence of a pathogen, preventing R protein activation. Upon the detection of Avirulence (Avr) proteins by the LRR domain a conformational change may take place, alleviating inhibition imposed by the LIM domain. However,

as the LIM domain commonly serves as a protein-binding interface in animals (Schmeichel and Beckerle, 1994), it may function similarly in plants. In an alternative model, the LIM domain serves as a binding site for a distinct negative regulator of CHS3 activity in the absence of a pathogen, with this interaction being disrupted by Avr protein detection.

There is mounting evidence to suggest that the LIM domain functions in the repression of R protein activity in CHS3 in the absence of pathogens. However, the detailed biochemical mechanism of how this inhibition occurs and under what conditions is still unclear. The extent of the interactions between the LIM domain and the other domains in CHS3 is also not understood. Future structural analysis of CHS3 may lend precise insights into the functional role of its LIM domain.

MATERIALS AND METHODS

PLANT GROWTH CONDITIONS, MUTANT ISOLATION, AND PHENOTYPIC CHARACTERIZATION

Arabidopsis thaliana (ecotype Col-0) plants were grown under a 16-h light/8-h dark photoperiod on either mixed soil or Murashige and Skoog (MS) medium supplemented with 0.5% (w/v) sucrose and 3% (w/v) phytagel.

The *npr1-1* suppressor screen was previously described by Gao et al. (2008). Briefly, seeds from *npr1-1* plants containing the *pPR2-GUS* reporter gene were treated with EMS. The seeds from approximately 1300 M1 plants were grown on MS media, yielding approximately 26 000 M2 plants. Half of the seedlings from a given line were tested for a gain of *pPR2-GUS* reporter gene expression by GUS staining. Seeds were collected from the remaining plants of those lines displaying constitutive *pPR2-GUS* expression. The M2 plants of these lines were sprayed with an *H.a.* Noco2 suspension (50 000 spores/mL) and scored 7 days post-treatment.

RNA for *PR* gene expression analysis was extracted from 14-day-old seedlings grown on MS medium using the RNAiso reagent (Takara). Reverse transcription was done using M-MLV reverse transcriptase (Takara). Real-time PCR was undertaken with the Perfect Real-Time kit (Takara). The primers used to amplify *Actin-1* were 5′-CGATGAAGCTCAATCCAAACGA-3′ and 5′-CAGAGTCGAGCACAATACCG-3′, the primers used to amplify *PR-1* were 5′-GTAGGTGCTCTTGTTCTTCCC-3′ and 5′-CACATAATTCCCACGAGGATC-3′, and the primers used to amplify *PR-2* were 5′-GCTTCCTTCTTCAACCACACAGC-3′ and 5′-CGTTGATGTACCGGAATCTGAC-3′.

SA extraction and measurement were carried out using HPLC according to procedures described previously (Li et al., 1999).

MAP-BASED CLONING OF *snc6*/*chs3-2D*

Markers used for mapping were generated using the Monsanto *Arabidopsis* polymorphisms and Landsberg sequence collections (Jander et al., 2002), obtained from TAIR (www.arabidopsis.org). Both insertion–deletion and SNP markers were used. The primer sequences for T4H18 are 5′-gaagaatgataagtgggaaaagag-3′ and 5′-gcccatcttccaattacagtc-3′. The primer sequences for F17K4 are 5′-tctctcatagggttccttcc-3′ and 5′-agatggcttggtgttcagac-3′. The primer sequences for MPI7 are 5′-gtgaattccaattagaccgca-3′ and 5′-tccttgataccgaccggtga-3′. The primer sequences for SNP marker MVA7 are 5′-gtaaaacagaaccatgagggc-3′ (Col-F), 5′-gtaaaacagaaccatgagggg-3′ (L*er*-F), and a common reverse primer, 5′-ggcaaagaagcagtcttgag-3′. The primer sequences for SNP marker MRG7 are 5′-gtagccaaaagtatgacaag-3′ (Col-F), 5′-gtagccaaaagtatgacaag-3′ (L*er*-F), and a common reverse primer, 5′-gatttccttcttcaagtccgc-3′. The primer sequences used for sequencing *CHS3* in the *snc6* mutant were 5′-ttggcatattctgggaaacc-3′ (17890-F1), 5′-GCATACTGAGCTTAACAAGG-3′ (17890-R1), 5′-CTGACTTCTTCCCCATTAGC-3′ (17890-R5), 5′-CTGGACTCA ATTTTCCAAAGG-3′ (17890-F2), 5′-CTAAGAGGAGGATT CACTTCTTC-3′ (17890-R2), 5′-ACCGCCATACGAGAATTGC-3′ (17890-F6), 5′- GCATTCCAAAGATCATGAGG-3′ (17890-F3), 5′-ctatggctgcaaaacgaagg-3′ (17890-R3), and 5′-GGTGATGGAACT CCCAAATG-3′ (17890-F7).

MOLECULAR CLONING

The full-length *CHS3* gene including the promoter region but lacking the stop codon was PCR amplified from Col-0 genomic DNA and cloned into a pCAMBIA1305-GFP vector in-frame to the N terminus of GFP using *Kpn*I and *Bam*HI restriction sites. The *CHS3-GFP* expression clone was sequenced to confirm in-frame fusion. Transformation was done using the floral dip method (Clough and Bent, 1998), and transformants were selected on MS medium supplemented with 30 μg/mL hygromycin. One-week-old seedlings were used to prepare protoplasts and confocal microscopy was used to analyze GFP fluorescence as previously described (Yoo et al., 2007). The same procedure was carried out for *chs3-2D*.

REVERTANT SCREEN

To identify revertant mutations in *chs3-2D*, EMS was used to mutagenize seeds of *chs3-2D*. The M1 progeny were allowed to self-fertilize and the M2 seeds were collected from these plants. These seeds were divided into 216 pools each representing approximately 10 M1 plants. The M2 progeny were screened for wild type morphology. Genomic DNA was extracted from wild type-like progeny, PCR amplified with *CHS3* primers and sequenced using the BigDye® Direct Cycle Sequencing kit (Applied Biosystems). The obtained sequence was compared with the wild type *CHS3* sequence to search for mutations. The primer sequences used were 5′-attctaattttaattgtcaaacac-3′ (At5g17890-F1), 5′-CCACTGATTATGATGCTTCTTG-3′ (At5g17890-F2), 5′-aagtctgggtatttatctgcaac-3′ (At5g17890-F3), 5′-TCAGTATGTGGGC TCATGAAG-3′ (At5g17890-F4), 5′-TTCTCATGATGGTGATGGA AC-3′ (At5g17890-F5), 5′-GCAAACACTTGTTTATCAACG-3′ (At5g17890-R1), 5′-CCCTGAGAAACATTTGATCTCTG-3′ (At5g 17890-R2), 5′-ATCTTACCTTACTTGACGTACTAG-3′ (At5g1789 0-R3), 5′-ATACATTCTCGACATAGCCATC-3′ (At5g17890-R4), and 5′-ctataacaaacattttagcttcg-3′ (At5g17890-R5).

ACKNOWLEDGMENTS

We would like to thank Oliver Dong and Virginia Woloshen for careful reading of the manuscript. This work was supported by grants from the Chinese Ministry of Science and Technology to Yuelin Zhang and from the National Science and Engineering Research Council (NSERC) to Xin Li. Kaeli C. M. Johnson is supported by an NSERC Alexander Graham Bell Canada Graduate Scholarship (M).

REFERENCES

Aarts, N., Metz, M., Holub, E., Staskawicz, B. J., Daniels, M. J., and Parker, J. E. (1998). Different requirements for EDS1 and NDR1 by disease resistance genes define at least two R gene-mediated signaling pathways in *Arabidopsis*. *Proc. Natl. Acad. Sci. U.S.A.* 95, 10306–10311.

Arber, S., and Caroni, P. (1996). Specificity of single LIM motifs in targeting and LIM/LIM interactions in situ. *Genes Dev.* 10, 289–300.

Baltz, R., Evrard, J. L., Bourdon, V., and Steinmetz, A. (1996). The pollen-specific LIM protein PLIM-1 from sunflower binds nucleic acids in vitro. *Sex. Plant Reprod.* 9, 264–268.

Bendahmane, A., Famham, G., Moffett, P., and Baulcombe, D. C. (2002). Consitutive gain-of-function mutants in a nucleotide binding site-leucine rich repeat protein encoded at the Rx locus of potato. *Plant J.* 32, 195–204.

Bernoux, M., Ve, T., Williams, S., Warren, C., Hatters, D., Valkov, E., Zhang, X., Ellis, J. G., Kobe, B., and Dodds, P. N. (2011). Structural and functional analysis of a plant resistance protein TIR domain reveals interfaces for self-association, signaling, and autoregulation. *Cell Host Microbe* 9, 200–211.

Bi, D., Cheng, Y. T., Li, X., and Zhang, Y. (2010). Activation of plant immune responses by a gain-of-function mutation in an atypical receptor-like kinase. *Plant Physiol.* 153, 1771–1779.

Bowling, S. A., Clarke, J. D., Liu, Y., Klessig, D. F., and Dong, X. (1997). The cpr5 mutant of *Arabidopsis* expresses both NPR1-dependent and NPR1-independent resistance. *Plant Cell* 9, 1573–1584.

Burch-Smith, T. M., Schiff, M., Caplan, J. L., Tsao, J., Czymmek, K., and Dinesh-Kumar, S. P. (2007). A novel role for the TIR domain in association with pathogen-derived elicitors. *PLoS Biol.* 5, e68. doi:10.1371/journal.pbio.0050068

Cao, H., Bowling, S. A., Gordon, A. S., and Dong, X. (1994). Characterization of an *Arabidopsis* mutant that is nonresponsive to inducers of systemic acquired resistance. *Plant Cell* 6, 1583–1592.

Cheng, Y. T., Germain, H., Wiermer, M., Bi, D., Xu, F., García, A. V., Wirthmueller, L., Després, C., Parker, J. E., Zhang, Y., and Li, X. (2009). Nuclear pore complex component MOS7/Nup88 is required for innate immunity and nuclear accumulation of defense regulators in *Arabidopsis*. *Plant Cell* 21, 2503–2516.

Clough, S. J., and Bent, A. F. (1998). Floral dip: a simplified method for Agrobacterium-mediated transformation of *Arabidopsis thaliana*. *Plant J.* 16, 735–743.

Dangl, J. L., and Jones, J. D. G. (2001). Plant pathogens and integrated defence responses to infection. *Nature* 411, 826–833.

Dodds, P. N., Lawrence, G. J., and Ellis, J. G. (2001). Six amino acid changes confined to the leucine-rich repeat beta-strand/beta-turn motif determine the difference between the P and P2 rust resistance specificities in flax. *Plant Cell* 13, 163–178.

Dong, X. (2004). NPR1, all things considered. *Curr. Opin. Plant Biol.* 7, 547–552.

Eliasson, A., Gass, N., Mundel, C., Baltz, R., Kräuter, R., Evrard, J. L., and Steinmetz, A. (2000). Molecular and expression analysis of a LIM protein gene family from flowering plants. *Mol. Gen. Genet.* 264, 257–267.

Ellis, J. G., Lawrence, G. J., Luck, J. E., and Dodds, P. N. (1999). Identification of regions in alleles of the flax rust resistance gene L that determine differences in gene-for-gene specificity. *Plant Cell* 11, 495–506.

Feuerstein, R., Wang, X., Song, D., Cooke, N. E., and Liebhaber, S. A. (1994). The LIM/double zinc-finger motif functions as a protein dimerization domain. *Proc. Natl. Acad. Sci. U.S.A.* 91, 10655–10659.

Feys, B. J., Wiermer, M., Bhat, R. A., Moisan, L. J., Medina-Escobar, N., Neu, C., Cabral, A., and Parker, J. E. (2005). *Arabidopsis* SENESCENCE-ASSOCIATED GENE101 Stabilizes and Signals within an ENHANCED DISEASE SUSCEPTIBILITY1 Complex in Plant Innate Immunity. *Plant Cell* 17, 2601–2613.

Freyd, G., Kim, S. K., and Horvitz, H. R. (1990). Novel cysteine-rich motif and homeodomain in the product of the *Caenorhabditis elegans* cell lineage gene lin-11. *Nature* 344, 876–879.

Frost, D., Way, H., Howles, P., Luck, J., Manners, J., Hardham, A., Finnegan, J., and Ellis, J. (2004). Tobacco transgenic for the flax rust resistance gene L expresses allele-specific activation of defense responses. *Mol. Plant Microbe Interact.* 17, 224–232.

Gao, M., Liu, J., Bi, D., Zhang, Z., Cheng, F., Chen, S., and Zhang, Y. (2008). MEKK1, MKK1/MKK2 and MPK4 function together in a mitogen-activated protein kinase cascade to regulate innate immunity in plants. *Cell Res.* 18, 1190–1198.

Garvalov, B. K., Higgins, T. E., and Sutherland, J. D. (2003). The conformational state of Tes regulates its zyxin-dependent recruitment to focal adhesions. *J. Cell Biol.* 161, 33–39.

Hammond-Kosack, K. E., and Jones, J. D. (1996). Resistance gene-dependent plant defense responses. *Plant Cell* 8, 1773–1791.

Horton, P., Park, K. J., Obayashi, T., Fujita, N., Harada, H., Adams-Collier, C. J., and Nakai, K. (2007). WoLF PSORT: protein localization predictor. *Nucleic Acids Res.* 35, W585–W587.

Huang, X., Li, J., Bao, F., Zhang, X., and Yang, S. (2010). A gain-of-function mutation in the *Arabidopsis* disease resistance gene RPP4 confers sensitivity to low temperature. *Plant Physiol.* 154, 796–809.

Hwang, C. F., Bhakta, A. V., Truesdell, G. M., Pudlo, W. M., and Williamson, V. M. (2000). Evidence for a role of the N terminus and leucine-rich repeat region of the Mi gene product in regulation of localized cell death. *Plant Cell* 12, 1319–1329.

Jander, G., Norris, S. R., Rounsley, S. D., Bush, D. F., Levin, I. M., and Last, R. L. (2002). *Arabidopsis* map-based cloning in the post-genome era. *Plant Physiol.* 129, 440–450.

Jones, J. D. G., and Dangl, J. L. (2006). The plant immune system. *Nature* 444, 323–329.

Kadrmas, J. L., and Beckerle, M. C. (2004). The LIM domain: from the cytoskeleton to the nucleus. *Nat. Rev. Mol. Cell Biol.* 5, 920–931.

Kim, H. S., and Delaney, T. P. (2002). *Arabidopsis* SON1 is an F-box protein that regulates a novel induced defense response independent of both salicylic acid and systemic acquired resistance. *Plant Cell* 14, 1469–1482.

Li, X., Clarke, J. D., Zhang, Y., and Dong, X. (2001). Activation of an EDS1-mediated R-gene pathway in the snc1 mutant leads to constitutive, NPR1-independent pathogen resistance. *Mol. Plant Microbe Interact.* 14, 1131–1139.

Li, X., Zhang, Y., Clarke, J. D., Li, Y., and Dong, X. (1999). Identification and cloning of a negative regulator of systemic acquired resistance, SNI1, through a screen for suppressors of npr1-1. *Cell* 98, 329–339.

Li, Y., Li, S., Bi, D., Cheng, Y. T., Li, X., and Zhang, Y. (2010). SRFR1 negatively regulates plant NB-LRR resistance protein accumulation to prevent autoimmunity. *PLoS Pathog.* 6, e1001111. doi:10.1371/journal.ppat.1001111

Li, Y., Zheng, L., Corke, F., Smith, C., and Bevan, M. W. (2008). Control of final seed and organ size by the DA1 gene family in *Arabidopsis thaliana*. *Genes Dev.* 22, 1331–1336.

Meyers, B. C., Kozik, A., Griego, A., Kuang, H., and Michelmore, R. W. (2003). Genome-wide analysis of NBS-LRR-encoding genes in *Arabidopsis*. *Plant Cell* 15, 809–834.

Nagata, K., Ohashi, K., Yang, N., and Mizuno, K. (1999). The N-terminal LIM domain negatively regulates the kinase activity of LIM-kinase 1. *Biochem. J.* 1, 99–105.

Nishiya, N., Sabe, H., Nose, K., and Shibanuma, M. (1998). The LIM domains of hic-5 protein recognize specific DNA fragments in a zinc-dependent manner in vitro. *Nucleic Acids Res.* 26, 4267–4273.

Papuga, J., Hoffman, C., Dieterle, M., Moes, D., Moreau, F., Tholl, S., Steinmetz, A., and Thomas, C. (2010). *Arabidopsis* LIM proteins: a family of actin bundlers with distinct expression patterns and modes of regulation. *Plant Cell* 22, 3034–3052.

Rairdan, G. J., Collier, S. M., Sacco, M. A., Baldwin, T. T., Boettrich, T., and Moffett, P. (2008). The coiled-coil and nucleotide binding domains of the potato Rx disease resistance protein function in pathogen recognition and signaling. *Plant Cell* 20, 739–751.

Rairdan, G. J., and Delaney, T. P. (2002). Role of salicylic acid and NIM1/NPR1 in race-specific resistance in *Arabidopsis*. *Genetics* 161, 803–811.

Rairdan, G. J., and Moffett, P. (2006). Distinct domains in the ARC region of the potato resistance protein Rx mediate LRR binding and inhibition of activation. *Plant Cell* 18, 2082–2093.

Rost, B., Yachdav, G., and Liu, J. (2003). The PredictProtein server. *Nucleic Acids Res.* 32, W321–W326.

Schmeichel, K. L., and Beckerle, M. C. (1994). The LIM domain is a modular protein-binding interface. *Cell* 79, 211–219.

Shah, J., Kachroo, P., and Klessig, D. F. (1999). The *Arabidopsis* ssi1 mutation restores pathogenesis-related gene expression in npr1 plants and renders defensin gene expression salicylic acid dependent. *Plant Cell* 11, 191–206.

Shah, J., Kachroo, P., Nandi, A., and Klessig, D. F. (2001). A recessive mutation in the *Arabidopsis* SSI2 gene confers SA- and NPR1-independent expression of PR genes and resistance against bacterial and oomycete pathogens. *Plant J.* 25, 563–574.

Shen, Q. H., Saijo, Y., Mauch, S., Biskup, C., Bieri, S., Keller, B., Seki, H., Ülker, B., Somssich, I. E., and Schulze-Lefert, P. (2007). Nuclear activity of MLA immune receptors links isolate-specific and basal disease-resistance responses. *Science* 315, 1098–1103.

Shen, Q. H., Zhou, F., Bieri, S., Haizel, T., Shirasu, K., and Schulze-Lefert, P. (2003). Recognition specificity and RAR1/SGT1 dependence in barley Mla disease resistance genes to the powdery mildew fungus. *Plant Cell* 15, 732–744.

Shirano, Y., Kachroo, P., Shah, J., and Klessig, D. (2002). A gain-of-function mutation in an *Arabidopsis* Toll Interleukin 1 receptor-nucleotide binding site-leucine-rich repeat type R gene triggers defense responses and results in enhanced disease resistance. *Plant Cell* 14, 3149–3162.

Swiderski, M. R., Birker, D., and Jones, J. D. G. (2009). The TIR Domain of TIR-NB-LRR resistance proteins is a signaling domain involved in cell death induction. *Mol. Plant Microbe Interact.* 22, 157–165.

Tameling, W. I. L., Vossen, J. H., Albrecht, M., Lengauer, T., Berden, J. A., Haring, M. A., Cornelissen, B. J., and Takken, F. L. (2006). Mutations in the NB-ARC domain of I-2 that impair ATP hydrolysis cause autoactivation. *Plant Physiol.* 140, 1233–1245.

Weaver, L. M., Swiderski, M. R., Li, Y., and Jones, J. D. (2006). The *Arabidopsis thaliana* TIR-NB-LRR R-protein, RPP1A; protein localization and constitutive activation of defence by truncated alleles in tobacco and *Arabidopsis*. *Plant J.* 47, 829–840.

Wirthmueller, L., Zhang, Y., Jones, J. D., and Paker, J. E. (2007). Nuclear accumulation of the *Arabidopsis* immune receptor RPS4 is necessary for triggering EDS1-dependent defense. *Curr. Biol.* 17, 2023–2029.

Yang, H., Shi, Y., Liu, J., Guo, L., Zhang, X., and Yang, S. (2010). A mutant CHS3 protein with TIR-NB-LRR-LIM domains modulates growth, cell death and freezing tolerance in a temperature-dependent manner in *Arabidopsis*. *Plant J.* 63, 283–296.

Yoo, S. D., Cho, Y. H., and Sheen, J. (2007). *Arabidopsis* mesophyll protoplasts: a versatile cell system for transient gene expression analysis. *Nat. Protoc.* 2, 1565–1572.

Zhang, Y., Yang, Y., Fang, B., Gannon, P., Ding, P., Li, X., and Zhang, Y. (2010). *Arabidopsis* snc2-1D activates receptor-like protein-mediated immunity transduced through WRKY70. *Plant Cell* 22, 3153–3163.

Zhou, F., Menke, F. L. H., Yoshioka, K., Moder, W., Shirano, Y., and Klessig, D. F. (2004). High humidity suppresses ssi4-mediated cell death and disease resistance upstream of MAP kinase activation, H_2O_2 production and defense gene expression. *Plant J.* 39, 920–932.

Zipfel, C., and Felix, G. (2005). Plants and animals: a different taste for microbes? *Curr. Opin. Plant Biol.* 8, 353–360.

Conflict of Interest Statement: The authors declare that the research was conducted in the absence of any commercial or financial relationships that could be construed as a potential conflict of interest.

Received: 04 July 2011; accepted: 14 October 2011; published online: 31 October 2011.

Citation: Bi D, Johnson KCM, Zhu Z, Huang Y, Chen F, Zhang Y and Li X (2011) Mutations in an atypical TIR-NB-LRR-LIM resistance protein confer autoimmunity. Front. Plant Sci. ***2****:71. doi: 10.3389/fpls.2011.00071*

This article was submitted to Frontiers in Plant-Microbe Interaction, a specialty of Frontiers in Plant Science.

APPENDIX

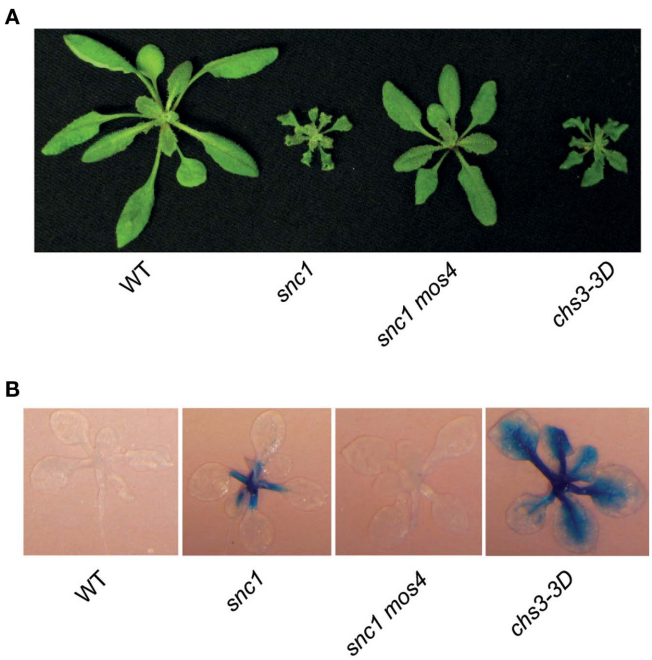

FIGURE A1 | Characterization of *chs3-3D*. (A) Morphology of WT, *snc1*, *snc1 mos4*, and *chs3-3D* soil-grown plants. Representative plants were photographed 4 weeks after germination. **(B)** Expression of the *pPR2-GUS* reporter gene, present in WT and *snc1* mutant background, in the above-mentioned genotypes. Seedlings were grown on MS media for 14 days prior to staining for GUS activity. The three photographs shown were taken at different magnifications in order to effectively capture GUS staining, thus seedling size should not be compared between panels.